Electronic Supplementary Material (ESI) for New Journal of Chemistry.

Synthesis, structure and phenoxazinone synthase-like activity of three unprecedented alternating Co^{II}–Co^{III} 1D chains

Sayantan Ganguly,[a,b] Paramita Kar,[a,c] Maharudra Chakraborty,[a] Koushik Sarkar,[d] Ashutosh Ghosh[a]*

[a]*Department of Chemistry, University College of Science, University of Calcutta, 92, A. P. C. Road, Kolkata-700 009, India; e-mail: ghosh_59@yahoo.com*

[b]*Department of Chemistry, Taki Government College, Taki, Hasnabad, West Bengal 743429, India*

[c]*Department of Chemistry, Bagnan College, Bagnan, Howrah, West Bengal 711303, India*

[d]*School of Chemical Sciences, Indian Association for the Cultivation of Science, 2A & 2B Raja S. C. Mullick Road, Kolkata 700032, India*

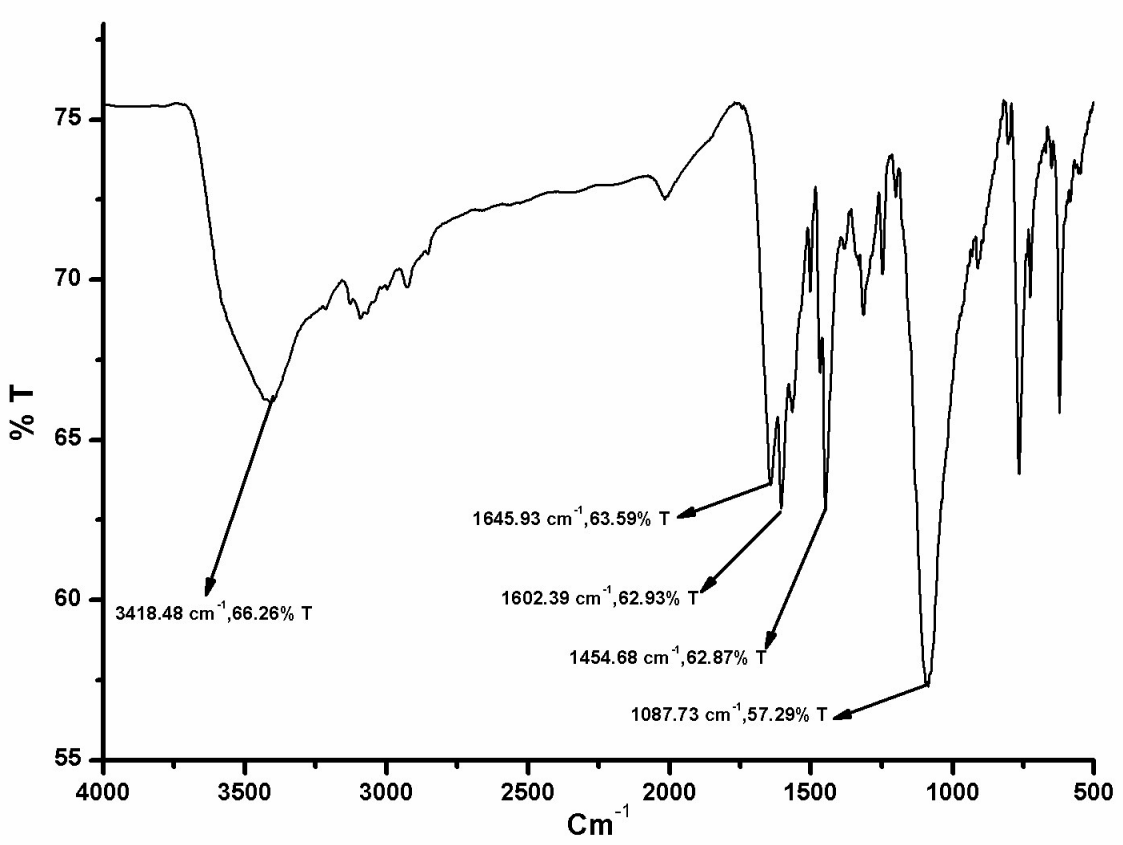

Fig. S1 Representative IR spectrum of complex **1**.

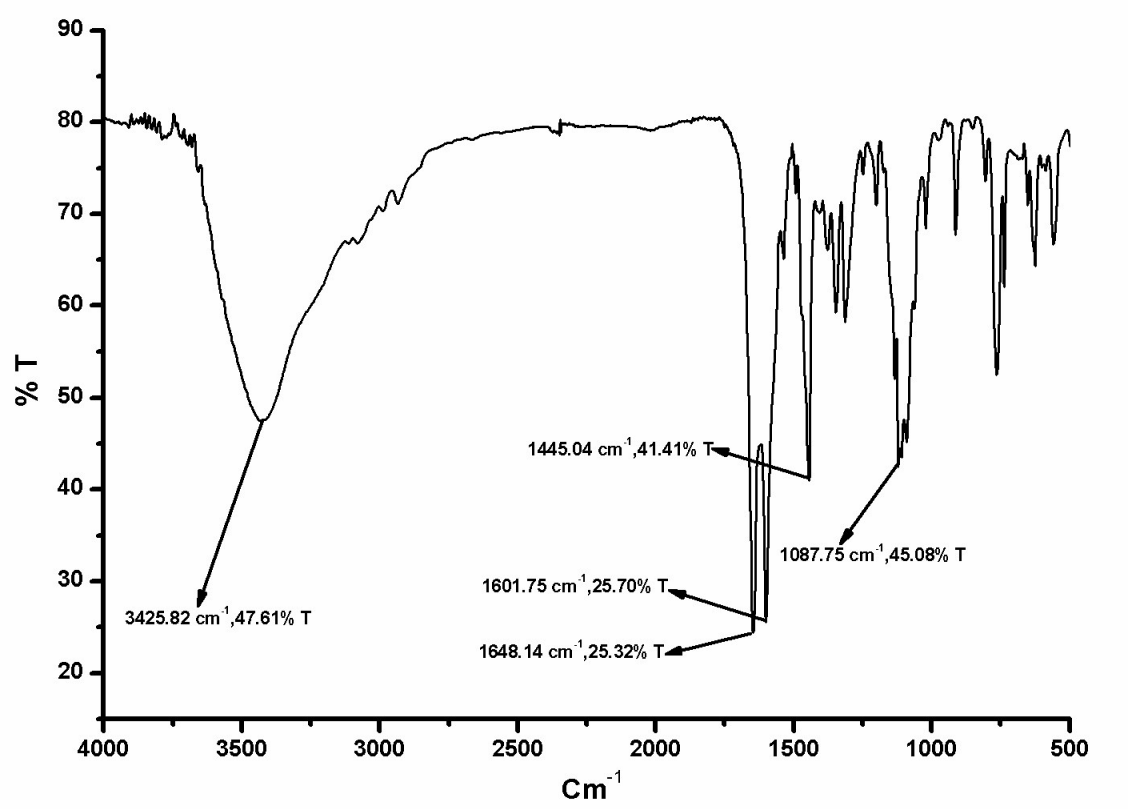

Fig. S2 Representative IR spectrum of complex **2**.

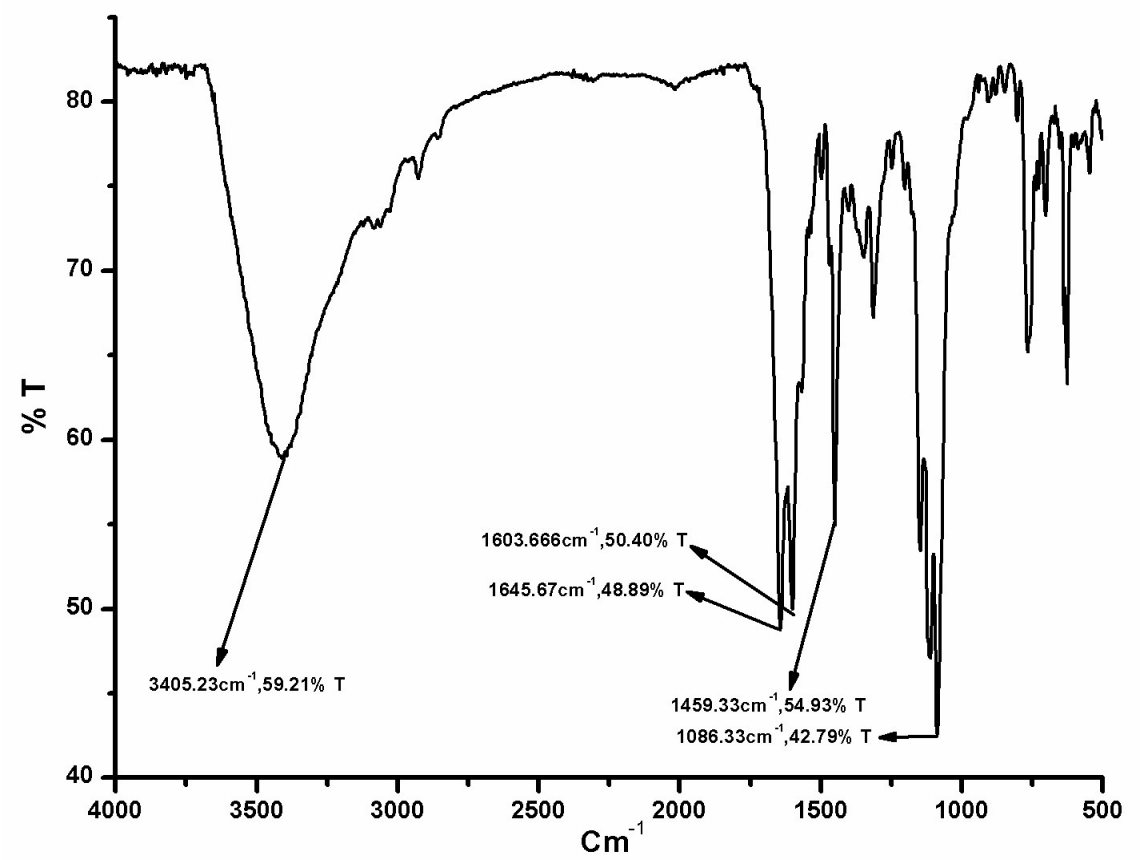

Fig. S3 Representative IR spectrum of complex **3**.

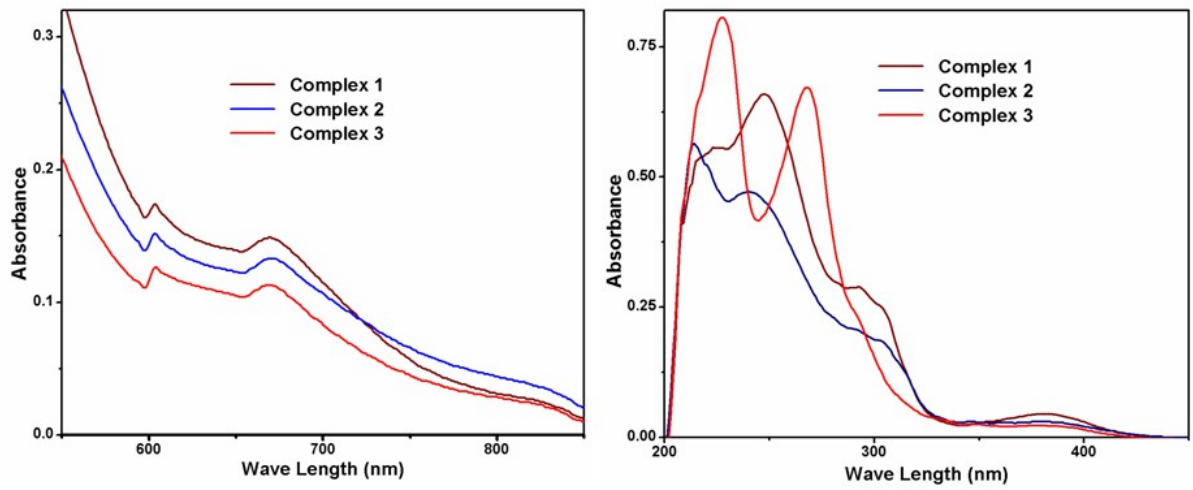

Fig. S4 Representative UV-Vis spectra of the complexes (**1**–**3**) in Methanol solution (left) d-d transition and (right) charge transfer band.

Table S1. Representation of the d-d band and CT band in the complexes (**1**–**3**)

Complex	d-d band (λ_{max}(nm) (ε,$M^{-1}cm^{-1}$) in CH_3OH)	CT band (λ_{max}(nm) (ε,$M^{-1}cm^{-1}$) in CH_3OH)
1	670 (152)	380(4000),246(65000),221(55000)
2	669 (136)	378(3226),241(47519),214(56960)
3	668 (114)	379(2419),267(67280),227(80386)

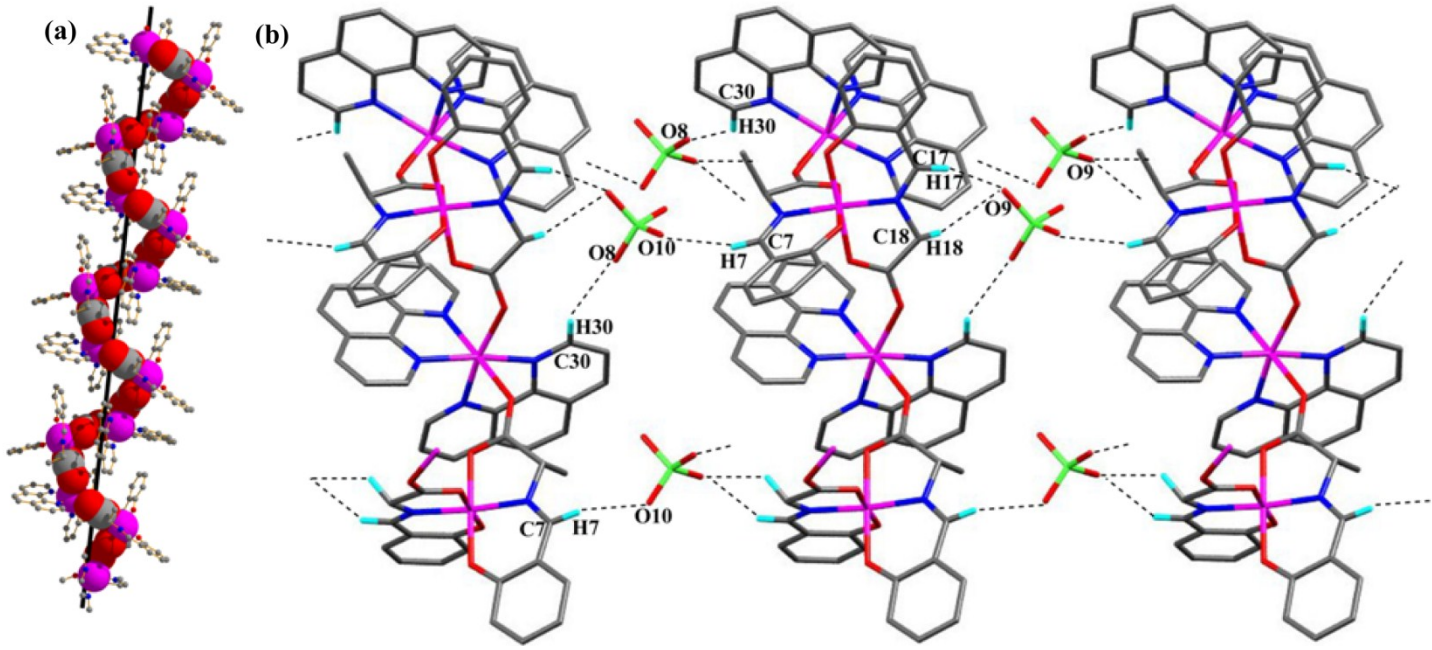

Fig. S5 (a) Helical polymeric structure along crystallographic b axis (Hydrogen atoms, anion and water molecule are omitted for clarity; (b) Formation of 2D supramolecular network by intermolecular hydrogen bonding interactions in complex **2**.

Table S2. Geometric features (Distances in (Å) and Angles in (^{0})) of the H-bond interactions obtained for complex 1

Donor–H·····Acceptor	D–H (Å)	H·····A (Å)	D·····A (Å)	∠D–H·····A (^{0})	Symmetry
C(7)–H(7)·····O(10A)	0.93	2.17	3.10(4)	173	-1+x,y,z

C(17)–H(17)·····O(9A)	0.93	2.54	3.32(4)	141	x, y, z
C(18)–H(18)·····O(8A)	0.98	2.53	3.41(3)	149	x, y, z
C(39)–H(39)·····O(8A)	0.93	2.54	3.37(5)	147	x, y, z
C(34)–H(34)·····O(7A)	0.93	2.43	3.31(3)	158	2-x, -1/2+y, 2-z

Table S3. Geometric features (Distances in (Å) and Angles in (^{0})) of the H-bond interactions obtained for complex 2

Donor–H·····Acceptor	**D–H (Å)**	**H·····A (Å)**	**D·····A (Å)**	**∠D–H·····A (^{0})**	**Symmetry**
C(7)–H(7)·····O(10)	0.95	2.41	3.28(19)	153	1+x, y, z
C(17)–H(17)·····O(9)	0.95	2.49	3.31(17)	144	x, y, z
C(18) –H(18)·····O(9)	1.00	2.54	3.26(19)	129	x, y, z
C(30)–H(30)·····O(8)	0.95	2.50	3.23(16)	134	1-x, -1/2+y, -z

Table S4. Geometric features (Distances in (Å) and Angles in (^{0})) of the H-bond interactions obtained for complex 3

Donor–H·····Acceptor	**D–H (Å)**	**H·····A (Å)**	**D·····A (Å)**	**∠D–H·····A (^{0})**	**Symmetry**
C(19)–H(19A)·····O(1)	0.97	2.56	3.258(13)	128	-1/2+x, 3/2-y, 2-z
C(9)–H(9A)·····O(8)	0.97	2.58	3.271(13)	128	1/2+x, 3/2-y, 2-z

Table S5. Geometric features (Distances in (A^0) and Angles in (^{0})) of the C-H /π interactions obtained for complex 3

C–H·····Cg(Ring)	**H·····Cg (Å)**	**∠C–H·····Cg (^{0})**	**C·····Cg (Å)**	**Symmetry**
C(29)–H(29)·····Cg(1)	2.85	133	3.551(15)	-1/2+X,3/2-Y,-Z

C(22)–H(22)·····Cg(2)	2.76	134	3.465(14)	1/2+X, 3/2-Y, -Z

Cg(1) = C1─C2─C3─C4─C5─C6─

Cg(2) = C11─C12─C13─C14─C15─C16─

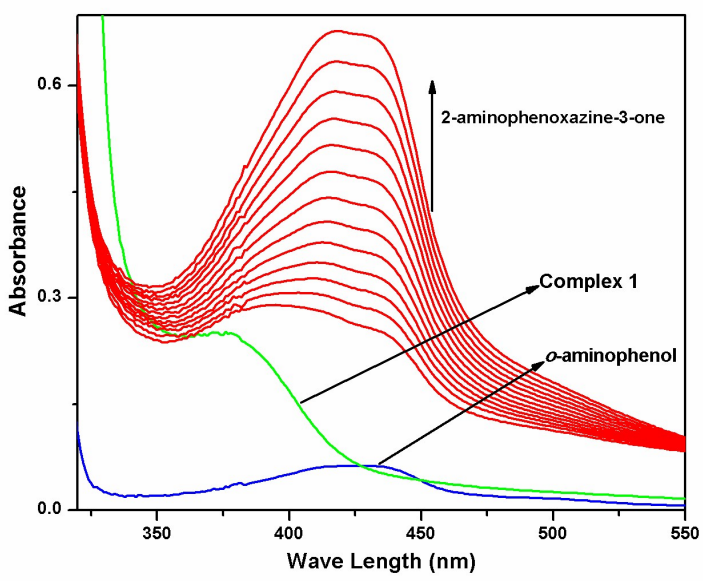

Fig. S6 Increase in absorbance around 430 nm, after mixing equal volumes of methanolic solutions of *o*-aminophenol (1.0 $\times 10^{-2}$ M) and **1** (1.0$\times$ 10^{-4} M). The spectra were recorded in every 5 min interval.

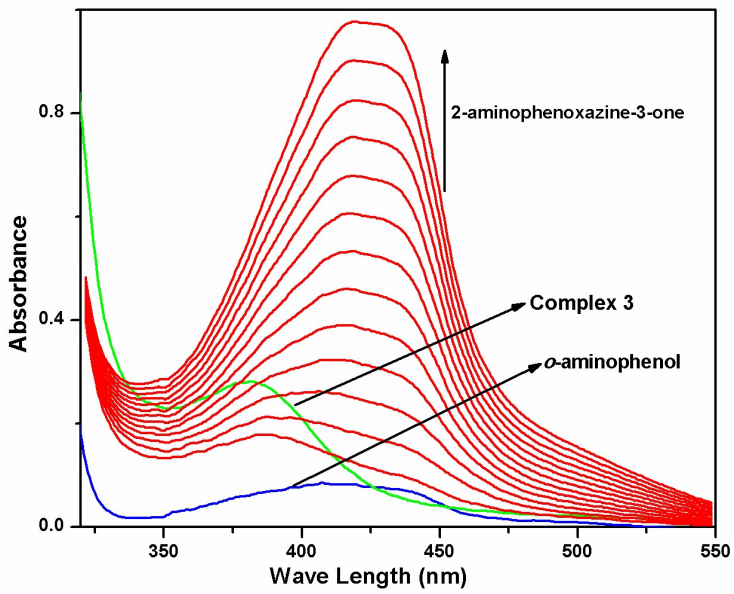

Fig. S7 Increase in absorbance around 430 nm, after mixing equal volumes of methanolic solutions of *o*-aminophenol (1.0 $\times 10^{-2}$ M) and **3** (1.0$\times$ 10^{-4} M). The spectra were recorded in every 5 min interval.

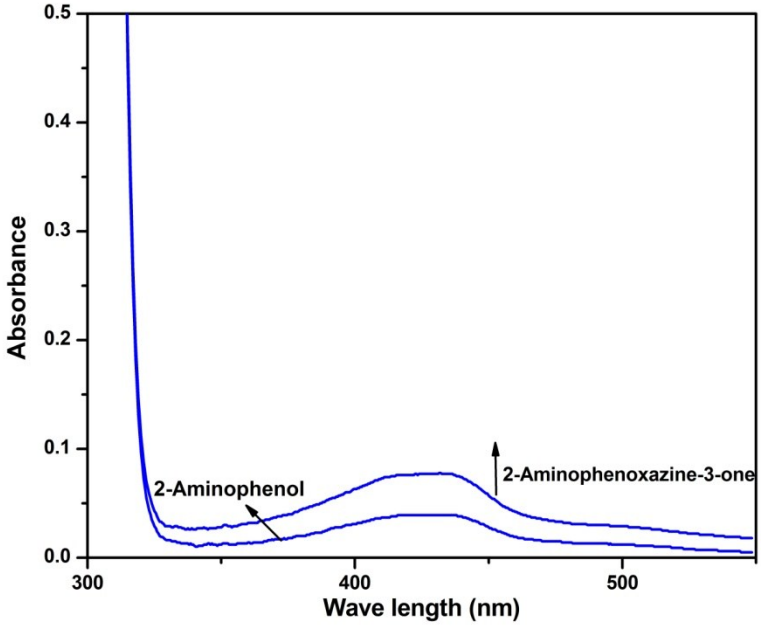

Fig. S8 Representative UV-Vis spectra of *o*-aminophenol (Blank).

Table S6. Different concentrations of substrate (*o*-aminophenol) in methanol for kinetic measurement

Metal complex and its concentration (M)	**Concentration of *o*-aminophenol (M)**
1(5.0×10^{-5})	5.0×10^{-4}, 1.5×10^{-3}, 2.5×10^{-3}, 3.5×10^{-3}, 5.0×10^{-3}, 7.5×10^{-3}, 1.0×10^{-2}, 1.3×10^{-2}, 1.5×10^{-2}
2(5.0×10^{-5})	5.0×10^{-4}, 1.5×10^{-3}, 2.5×10^{-3}, 3.5×10^{-3}, 5.0×10^{-3}, 7.5×10^{-3}, 1.0×10^{-2}, 1.3×10^{-2}, 1.5×10^{-2}, 2.0×10^{-2}, 2.5×10^{-2}, 3.0×10^{-2}
3(5.0×10^{-5})	5.0×10^{-4}, 1.5×10^{-3}, 2.5×10^{-3}, 3.5×10^{-3}, 5.0×10^{-3}, 7.5×10^{-3}, 1.0×10^{-2}, 1.3×10^{-2}

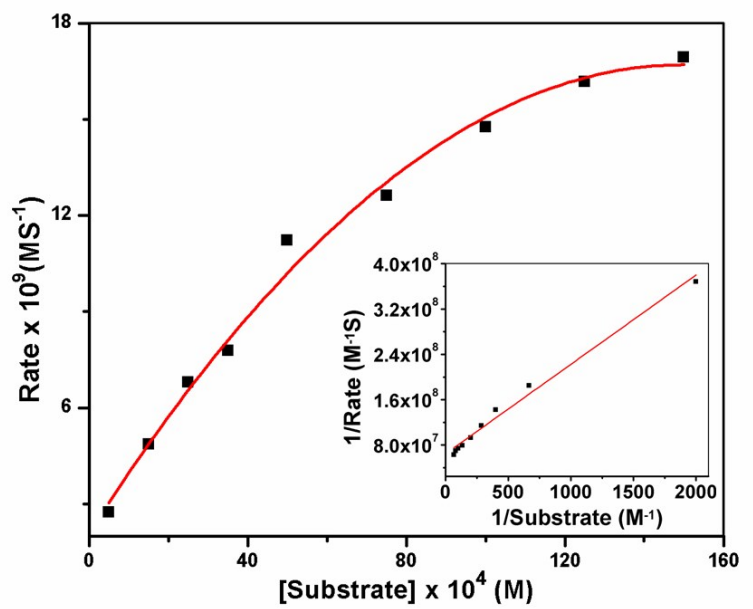

Fig. S9 Plot of initial rates *vs* substrate concentration for the oxidation reaction of *o*-amino phenol catalyzed by complex **1.** Inset shows the Lineweaver−Burk plot. Symbols and solid lines represent the experimental and simulated profiles, respectively.

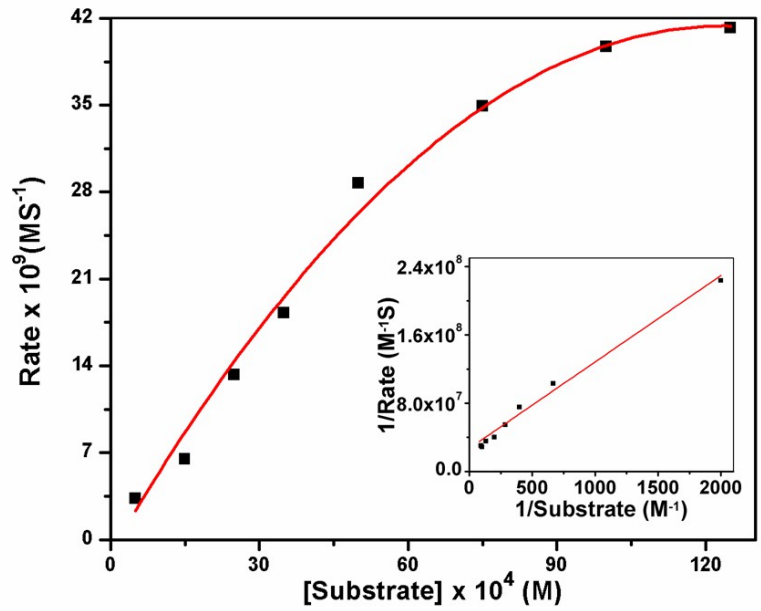

Fig. S10 Plot of initial rates *vs* substrate concentration for the oxidation reaction of *o*-amino phenol catalyzed by complex **3.** Inset shows the Lineweaver−Burk plot. Symbols and solid lines represent the experimental and simulated profiles, respectively.

Table S7. Kinetic parameters for phenoxazinone synthase activity of complexes (**1–3**)

Complex	V_{max} ($M\ S^{-1}$)	Std. Error	K_M (M)	Std. Error	k_{cat} (h^{-1})
1	1.59×10^{-8}	2.21×10^{-9}	2.66×10^{-3}	1.88×10^{-4}	1.2
2	1.60×10^{-7}	2.76×10^{-8}	1.81×10^{-2}	2.73×10^{-4}	11.5
3	3.69×10^{-8}	1.69×10^{-8}	3.74×10^{-3}	5.97×10^{-4}	2.7

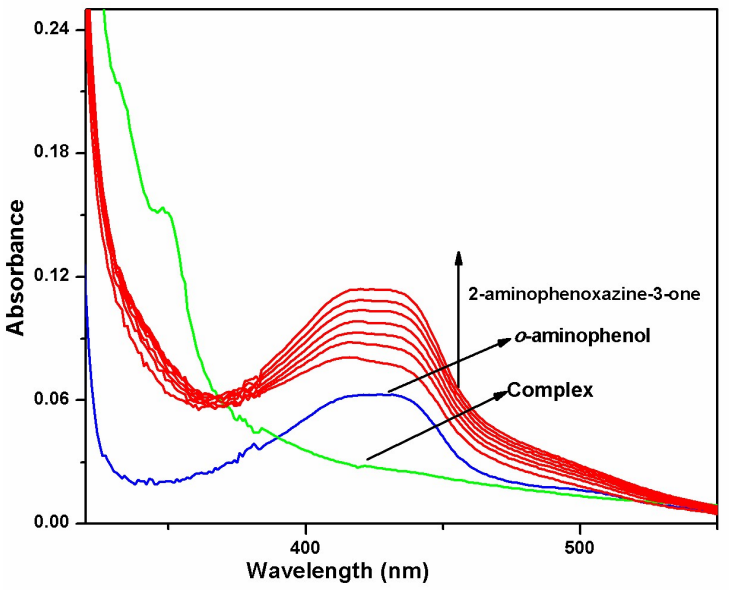

Fig. S11 Representative UV-Vis spectra of the complex $\{[Co^{II}(bpy)_3]\cdot(ClO_4)_2\cdot H_2O\}$ with *o*-amino phenol.

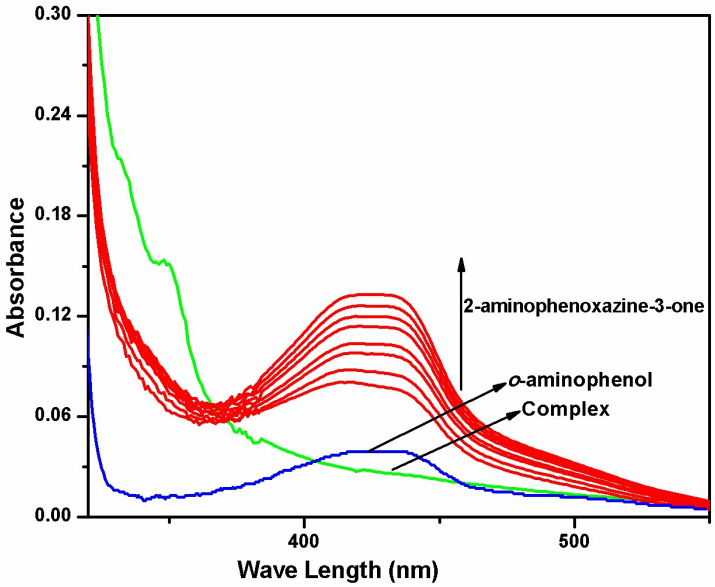

Fig. S12 Representative UV-Vis spectra of the complex $\{[Co^{II}(phen)_3]\cdot(ClO_4)_2\cdot H_2O\}$ with *o*-amino phenol.

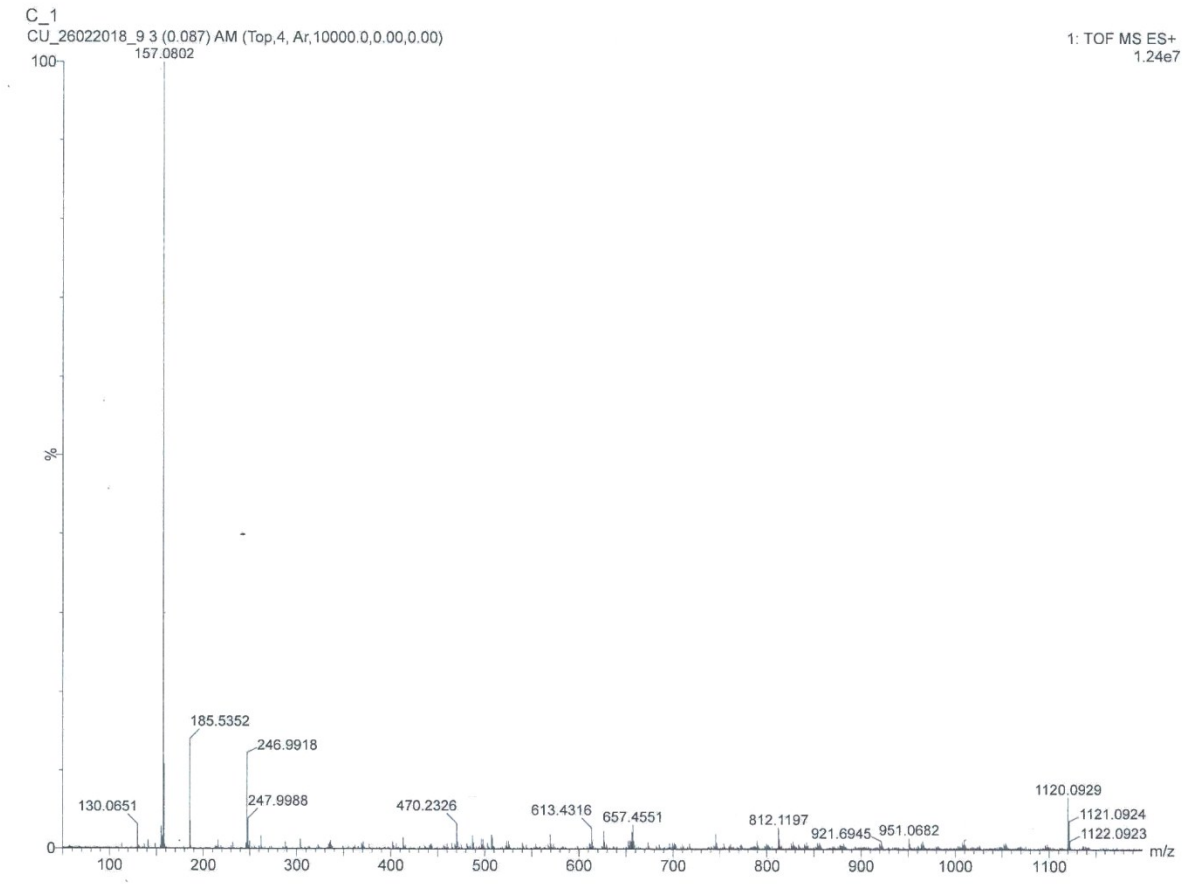

Fig. S13 Representative ESI mass spectrum of complex **1**.

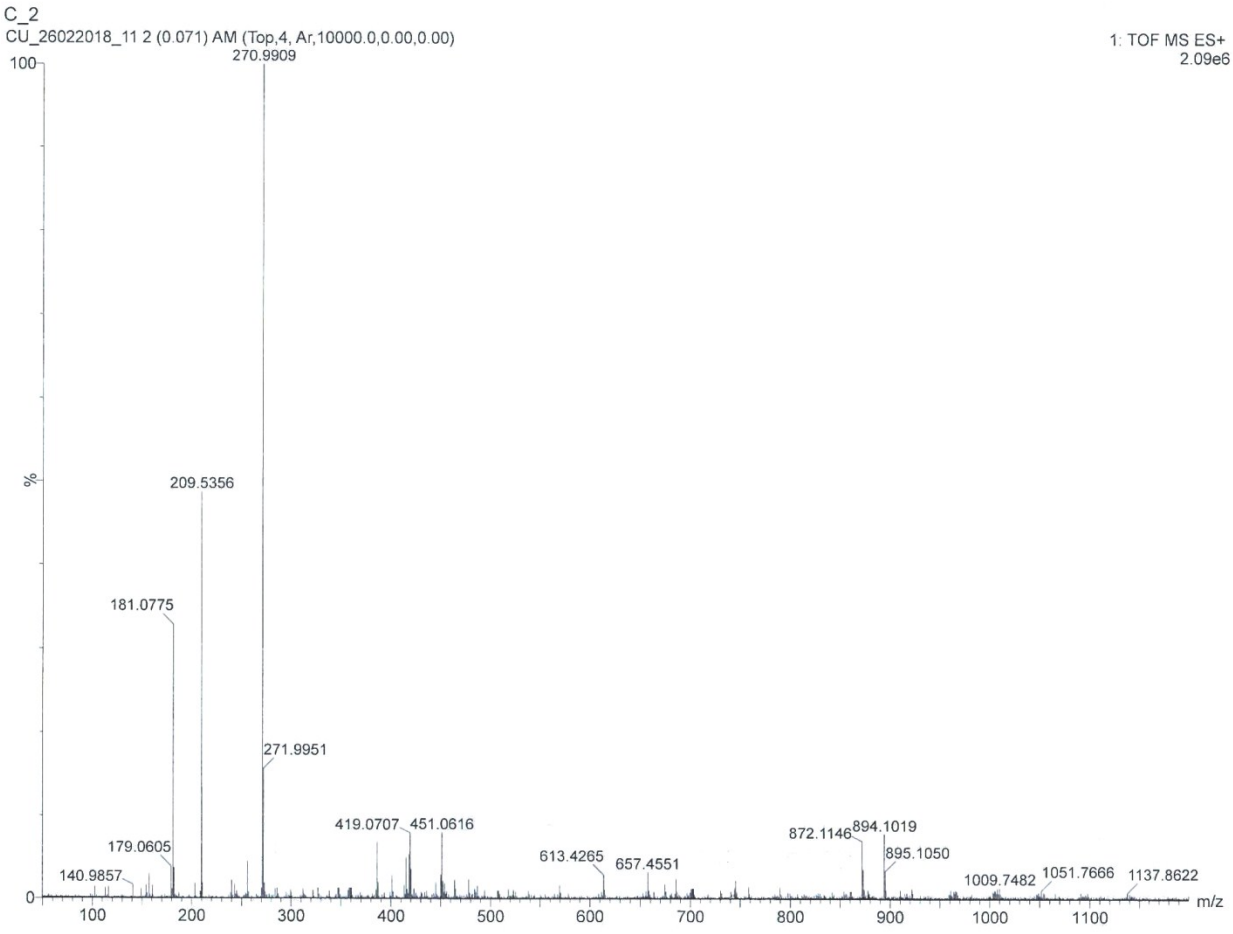

Fig. S14 Representative ESI mass spectrum of complex **2**.

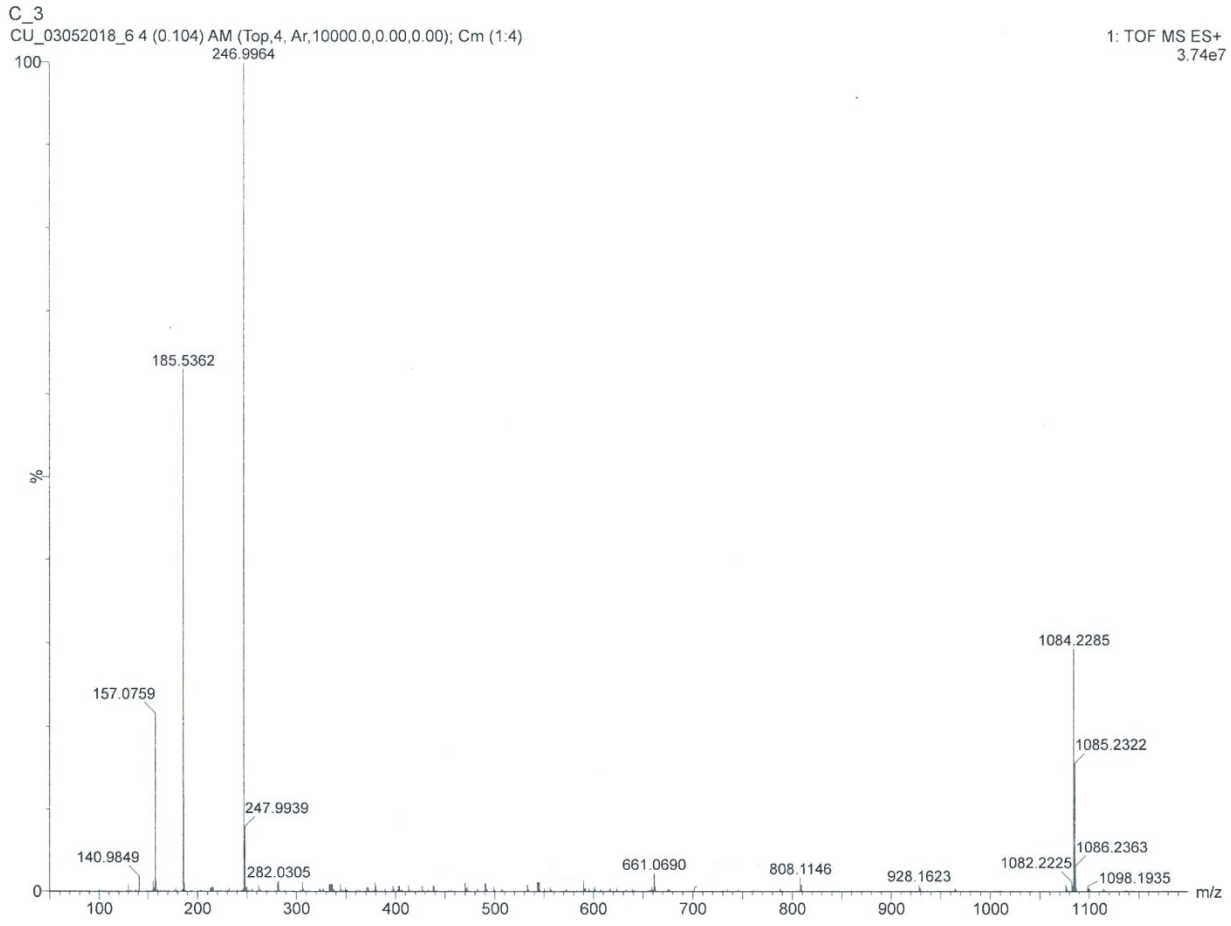

Fig. S15 Representative ESI mass spectrum of complex **3**.

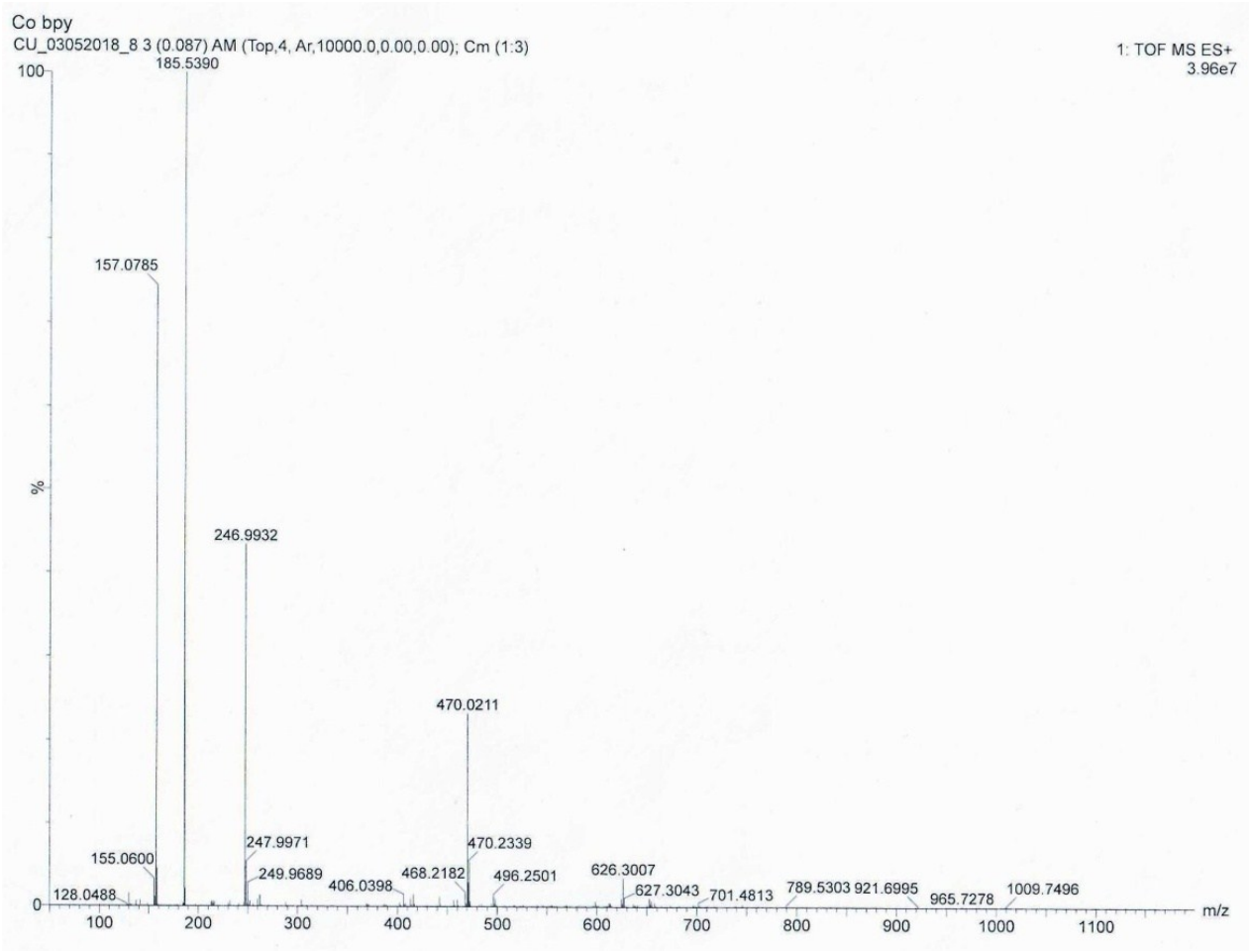

Fig. S16 Representative ESI mass spectrum of $\{[Co^{II}(bpy)_3]\cdot(ClO_4)_2\cdot H_2O\}$.

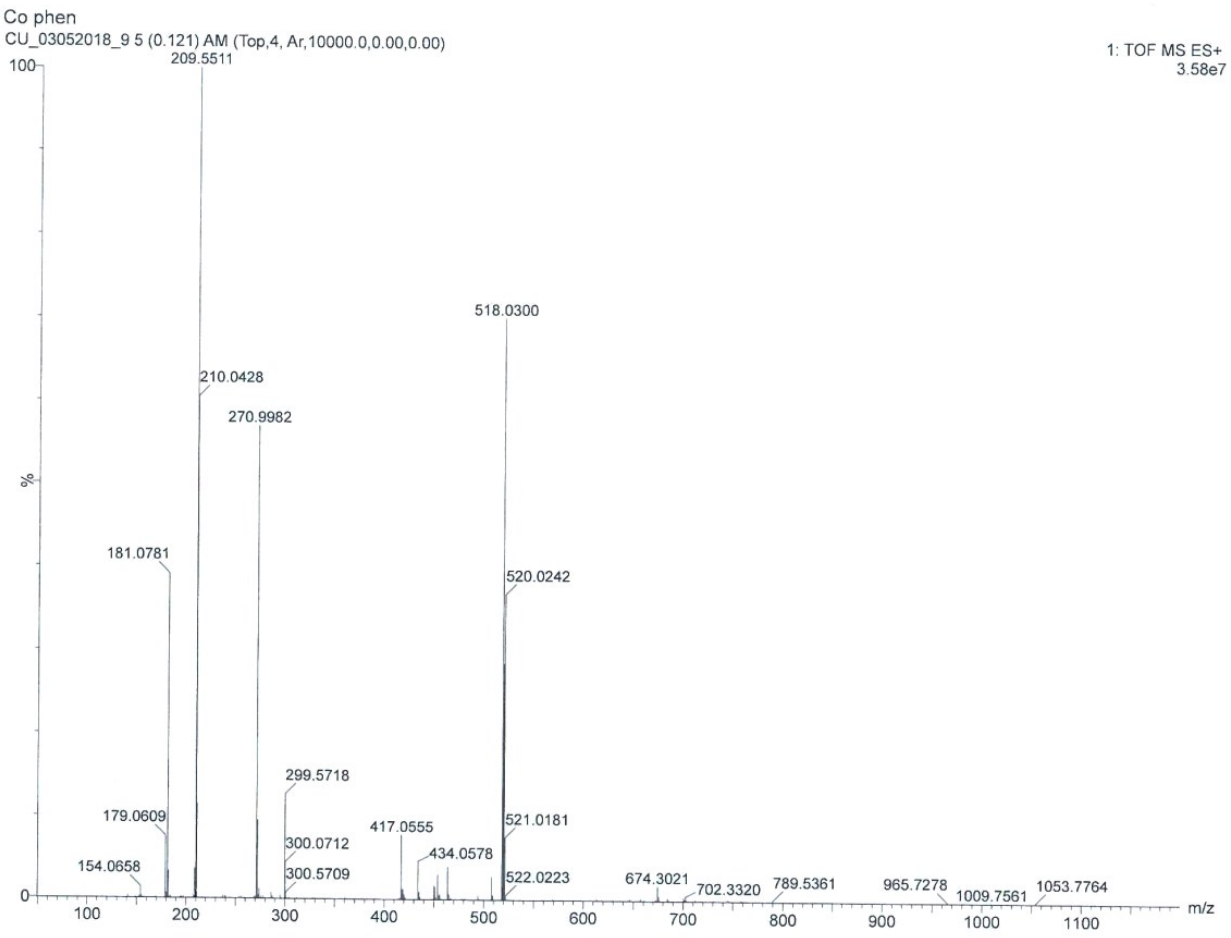

Fig. S17 Representative ESI mass spectrum of $\{[Co^{II}(phen)_3]\cdot(ClO_4)_2\cdot H_2O\}$.

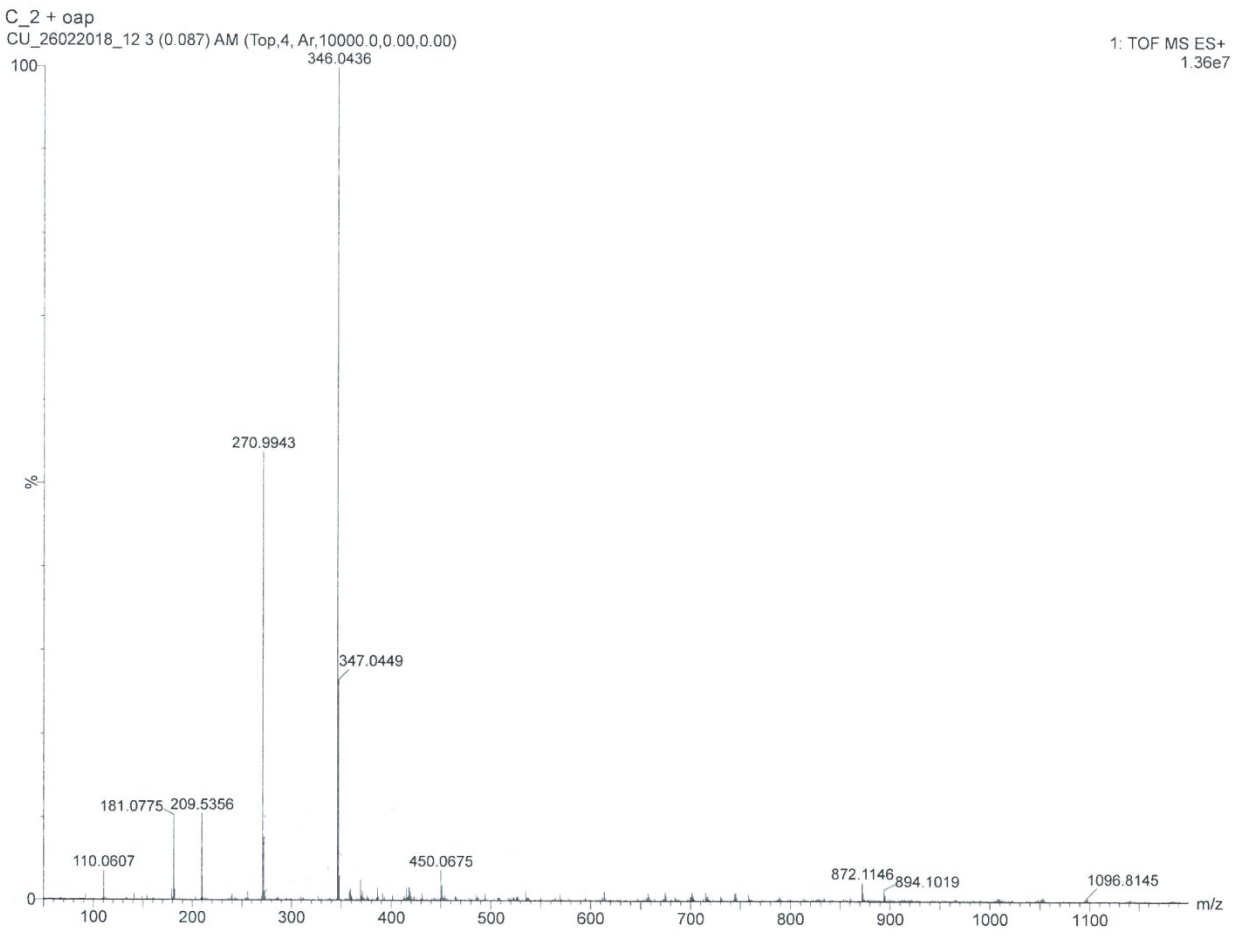

Fig. S18 Representative ESI mass spectrum of complex **2** with *o*-amino phenol.

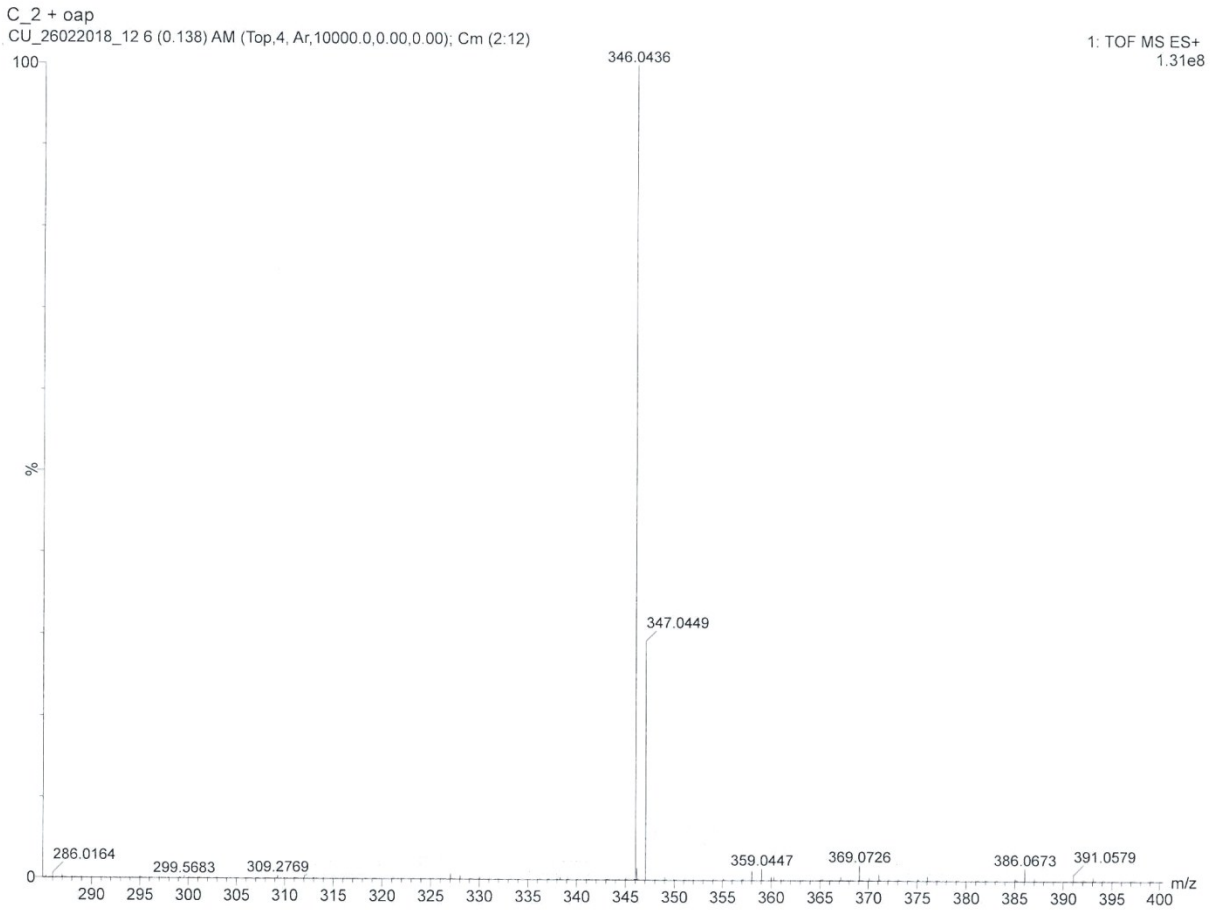

Fig. S19 Representative ESI mass spectrum of complex **2** with *o*-amino phenol (Expanded).

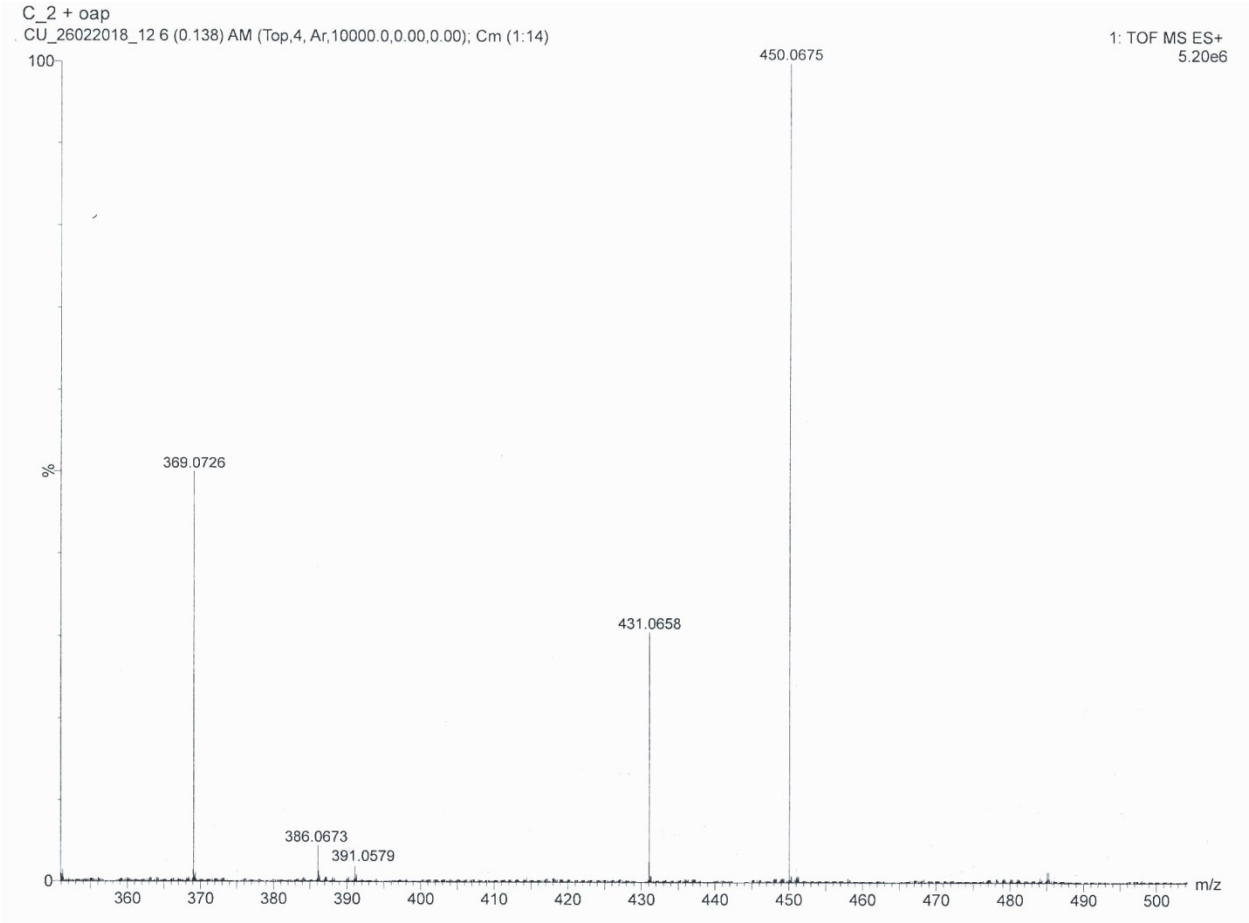

Fig. S20 Representative ESI mass spectrum of complex **2** with *o*-amino phenol (Expanded).

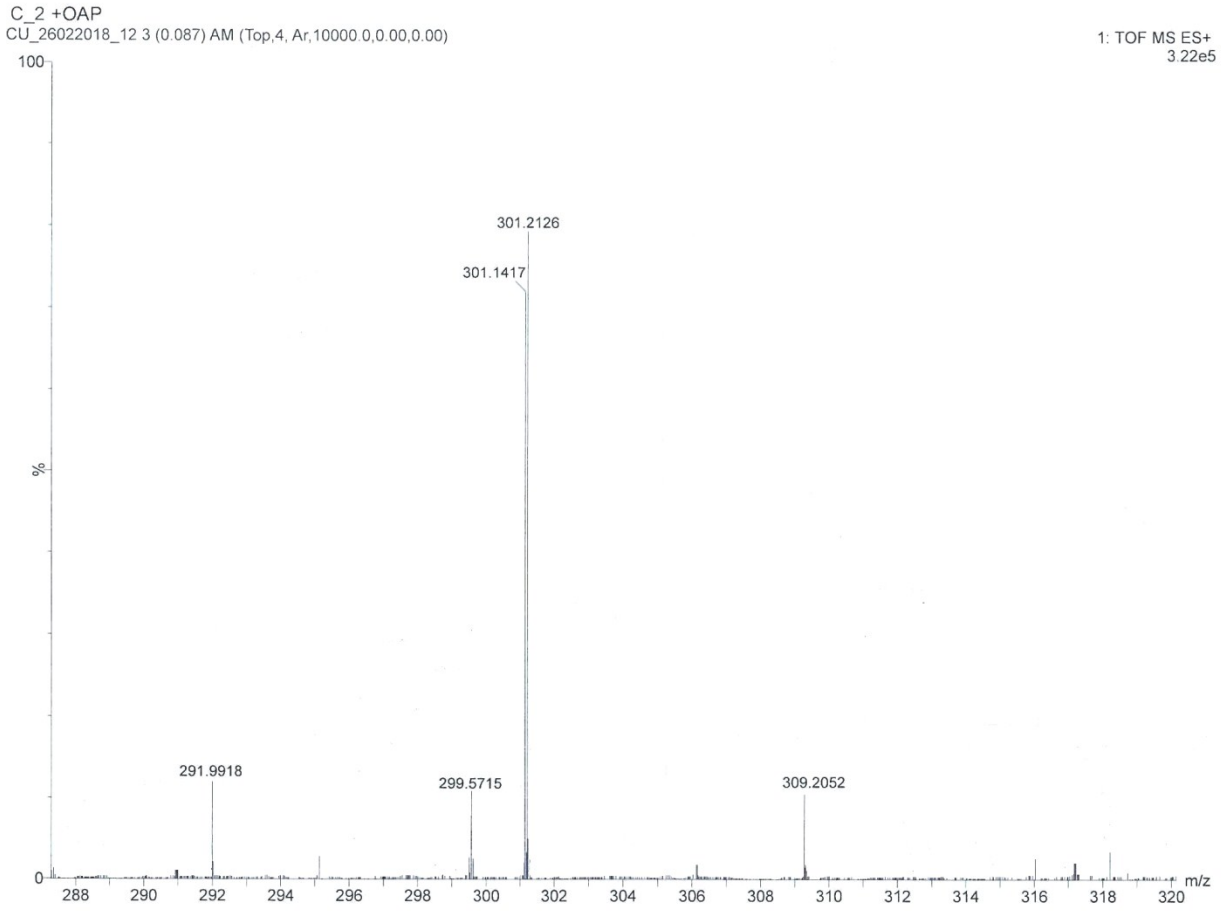

Fig. S21 Representative ESI mass spectrum of complex **2** with *o*-amino phenol (Expanded).

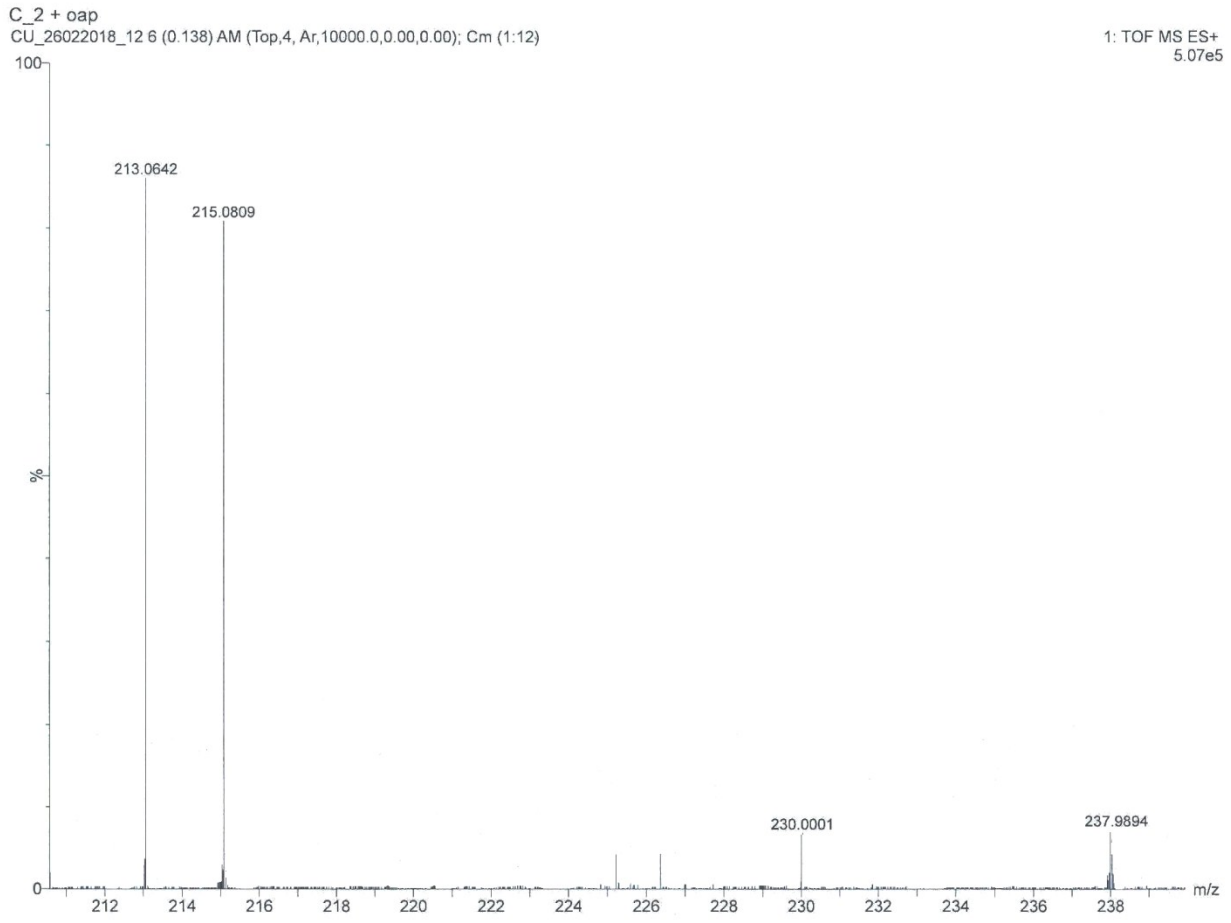

Fig. S22 Representative ESI mass spectrum of complex **2** with *o*-amino phenol (Expanded).

Table S8. k_{cat} Values for the oxidation of OAPH to 2-aminophenoxazine-3-one catalyzed by complex **1**, **2** and **3** and other reported cobalt complexes.[a]

	Complexes	k_{cat} (h^{-1}) in CH_3OH	k_{cat} (h^{-1}) in CH_3CN	k_{cat} (h^{-1}) in DMF	References
Co^{II} complexes	$[Co^{II}(Hdmg)L^1]$	Not Performed	Not Performed	Not Performed	14a
	$[Co^{II}(L^2)Cl(H_2O)]Cl.H_2O$	13.7	Not Performed	Not Performed	25a
	$[Co^{II}(L^2)(NCS)_2]$	7.4	Not Performed	Not Performed	25a
	$[Co^{II}(L^3)Cl_2]$	4.1	Not Performed	Not Performed	25a
	$[Co^{II}(L^4)(CH_3CN)](ClO_4)_2$	3.4	Not Performed	Not Performed	14b
	$[Co^{II}(L^5)(H_2O)](ClO_4)_2$	6.4	Not Performed	Not Performed	14b
	$[Co^{II}(L^6)(H_2O)](ClO_4)_2$	8.3	Not Performed	Not Performed	14b
	$[Co^{II}_4\ L^7{}_2(\mu_{1,1,1}\text{-}N_3)_2(N_3)_2]$	500.4	Not Performed	Not Performed	2d
	$[Co^{II}_4\ L^7{}_2(\mu_3\text{-}OH)_2(NCS)_2]\cdot 4CH_3CN$	508.9	Not Performed	Not Performed	2d
	$[Co^{II}_4\ L^7{}_2(\mu_3\text{-}OH)_2(NCSe)_2]\cdot 2CH_3CN$	511.2	Not Performed	Not Performed	2d
Co^{III} complexes	$[Co^{III}\ (L^8)_3]$	Not Performed	Not Performed	Not Performed	25b
	$[Co^{III}_2(L^9)_2(\mu\text{-}L^{10})_2Cl_2]\ Cl_2\cdot 2H_2O$	13.8	Not Performed	Not Performed	25c

	$[Co^{III}(L^{11})(N_3)_3]$	20.4	Not Performed	Not Performed	14c
	$[Co^{III}(L^{12})(N_3)_3]$	33.3	Not Performed	Not Performed	14c
	$[Co^{III}_2(L^{13})_2(\mu\text{-}O_2)](ClO_4)_4 \cdot 2CH_3CN$	30.1	Not Performed	Not Performed	14b
	$[Co^{III}_2(L^{14})_2(\mu\text{-}O_2)](ClO_4)_4$	23.4	Not Performed	Not Performed	14b
	$[L^{15}Co^{III}(L^{16})_2]ClO_4 \cdot CH_3OH \cdot H_2O$	11.5	Not Performed	Not Performed	25d
	$[L^{15}Co^{III}(L^{17})_2Na(ClO_4)_2] \cdot 0.5H_2O$	27.9	Not Performed	Not Performed	25d
	$[Co^{III}(L^{18})(N_3)_2].0.5CH_3CN$	54.0	Not Performed	Not Performed	14d
	$[Co^{III}(L^{18})(NCS)_2].0.5H_2O$	48.6	Not Performed	Not Performed	14d
	$[Co^{III}(L^{19})_2(py)_2]Cl \cdot 8H_2O$	30.6	Not Performed	Not Performed	25e
	$[L^{20}Co^{III}(L^{21})(H_2O)]ClO_4 \cdot CH_3OH$	45.1	Not Performed	Not Performed	25f
	$[L^{20}Co^{III}(L^{1})(H_2O)]PF_6$	54.0	Not Performed	Not Performed	25f
	$[Co^{III}(HL^{22})_2]OCOCH_3 \cdot H_2O$	28300	Not Performed	Not Performed	25g
	$[Co^{III}(HL^{23})_2](ClO_4)_3 \cdot 2H_2O$	4.4	Not Performed	Not Performed	14e
	$[Co^{III}(L^{23})\ (N_3)_2]$	56.0	Not Performed	Not Performed	14e
	$[Co^{III}(L^{23})\ (NCS)_2]$	53.8	Not Performed	Not Performed	14e

	$[Co^{III}(L^{24})(N_3)(L^{25})]$	29952	Not Performed	Not Performed	25h
	$[Co^{III}(L^{26})(bzan)(N_3)]$	Not Performed	14832	Not Performed	26a
	$[Co^{III}(L^{26})(bzan)(NCS)]$	Not Performed	15444	Not Performed	26a
	$[Co^{III}(L^{27})(L^{28})(N_3)]\cdot H_2O$	Not Performed	122.8	Not Performed	26b
	$[Co^{III}(L^{29})(L^{30})(NCS)]$	Not Performed	466.7	Not Performed	26b
	$[Co^{III}(L^{31})(acna)(N_3)]$	Not Performed	77.5	Not Performed	26c
	$[Co^{III}(L^{32})(bzan)(N_3)]$	Not Performed	77.1	Not Performed	26c
	$[Co^{III}L^{33}2]Cl$	9720.0	Not Performed	Not Performed	26d
	$[Co^{III}(HL^{34})2](ClO4)3\cdot 2H2O$	3.8	Not Performed	Not Performed	14f
	$[Co^{III}(L^{34})(N3)2]$	51.8	Not Performed	Not Performed	14f
	$[Co^{III}(L^{34})(NCS)2]$	48.4	Not Performed	Not Performed	14f
	$[Co^{III}(L^{35})(N_3)_2]$	47.4	Not Performed	Not Performed	14g
	$[Co^{III}(L^{35})(NCS)_2]$	47.6	Not Performed	Not Performed	14g
Mixed valence $Co^{II/III}$ complexes	$[(Co^{III})_2(Co^{II})L^{36}_2(\mu_2\text{-}PhCO_2^-)_2(PhCO_2^-)_2]$	Not Performed	153.6	Not Performed	14h
	$[Co^{III}(HL^{18})_2][Co^{II}(NCS)_4].NCS$	26.1	Not Performed	Not Performed	14d

	$[Co^{III}(L^{18})_2]_2[Co^{II}(NCO)_4]$	8.3	Not Performed	Not Performed	14d
	$[Co^{III}(HL^{23})(L^{23})][Co^{II}(NCS)_4].5CH_3OH$	20.7	Not Performed	Not Performed	14e
	$[Co^{III}(L^{23})_2]_2[Co^{II}(NCO)_4]$	30.0	Not Performed	Not Performed	14e
	$[Co^{III}(L^{34})(Br\text{-}sal)]_2[Co^{II}(NCS)_4]$	11.8	Not Performed	Not Performed	14f
	$[Co^{III}(L^{35})(sal)]_2[Co^{II}(NCS)_4]$	16.5	Not Performed	Not Performed	14g
	$[Co^{III}(L^{35})_2]_2[Co^{II}_{0.5}(NCS)_2][Co^{II}_{0.25}(NCS)]Cl_{0.5}$	10.3	Not Performed	Not Performed	14g
Mixed valence $Co^{II/III}$ coordination polymer	Complex **1**	1.2	Not Performed	Not Performed	Present Study
	Complex **2**	11.5	Not Performed	Not Performed	Present Study
	Complex **3**	2.7	Not Performed	Not Performed	Present Study

[a] Where L^1 = triphenyl phosphine, L^2 = N,N′-bis(pyridin-2-ylmethylene)-2,2-dimethylpropane-1,3-diamine, L^3 = N,N′-bis(6 methylpyridin-2-ylmethylene)-2,2-dimethylpropane-1,3-diamine, L^4 = N^1-(2-(methoxy(6-methylpyridin-2-yl)methylamino)propyl)-N^3-((6-methylpyridin-2-yl)methylene)propane-1,3-diamine, L^5 = N^1-(3-((6-methylpyridin-2-yl)methyleneamino)propyl)-N^3-((6-methylpyridin-2-yl)methylene)propane-1,3-diamine, L^6 = N^1-(3-((6-methylpyridin-2-yl)methyleneamino)propyl)-N^1-methyl-N^3-((6-methylpyridin-2-yl)methylene)propane-1,3-diamine, H_2L^7 = N,N′-dimethyl-N,N'-bis(2-hydroxy-3-methoxy-5-methylbenzyl)ethylenediamine, L^8 =4,4′-dimethyl-2,2′-bipyridine, L^9= 2-aminomethylpyridine, L^{10} = 2-iminomethylpyridine anion, L^{11} = Bis-(2-pyridylmethyl)amine, L^{12} = (2-pyridylmethyl)(2-pyridylethyl)amine, L^{13} = N^1-(3-((pyridin-2-yl)methyleneamino)propyl)-N^3-((pyridin-2-yl)methylene)propane-1,3-diamine, L^{14} = N^1 -(3-(1-(pyridin-2-

yl)ethylideneamino)propyl)-N^3-(1-(pyridin-2-yl)ethylidene)propane-1,3-diamine, H_2L^{15} = N,N′-bis(3-methoxysalicylidehydene)cyclohexane-1,2-diamine), L^{16}=4-aminopyridine, L^{17}=1-methylimidazole, HL^{18} = 2-((E)-(3-(3-(dimethylamino)propylamino)propylimino)methyl)-6-methoxyphenol, H_2L^{19} = 3,5,6-tribromo-4-pyridiniumcatechol, H_2L^{20}= N,N′-bis(3-methoxysalicylidehydene)cyclohexane-1,2-diamine, L^{21} = tri(*m*-tolyl)phosphine, H_2L^{22} = N-(2-hydroxyethyl)-3-methoxysalicylaldimine, HL^{23} = 2-((E)-(3-(3-(dimethylamino)propylamino)propylimino)methyl)-6-ethoxyphenol, HL^{24} = 1-((2-(diethylamino)ethylimino)methyl)naphthalene-2-ol, HL^{25} = acetylacetone, HL^{26} = 2-(3-(dimethylamino)propyliminomethyl)-6-ethoxyphenol, Hbzan = 1-benzoylacetone, HL^{27} = 2-((2-(piperidin-1-yl)ethylimino)methyl)-6-ethoxyphenol, HL^{28}=1-acetyl-2-naphthol, HL^{29} = 2-((3-(dimethylamino)propylimino)methyl)-6-methoxyphenol, HL^{30} = 2,4-pentanedione, HL^{31} = 2((2(2-hydroxyethylamino)ethylimino)methyl)-6-ethoxyphenol, Hacna = 2-acetyl-1-naphthol, HL^{32} = 1((2(diethylamino)ethylimino)methyl)naphthalen-2-ol, HL^{33} = 2-(3-aminopropylthio)ethanol, HL^{34} = 2-((E)-(3-(3-(dimethylamino)propylamino)propylimino)methyl)-4-bromophenol, HL^{35} = 2-((E)-(3-(3-(dimethylamino)propylamino)propylimino)methyl)phenol, H_2L^{36} = N,N'-bis(2-hydroxybenzyl)-1,3-propanediamine.

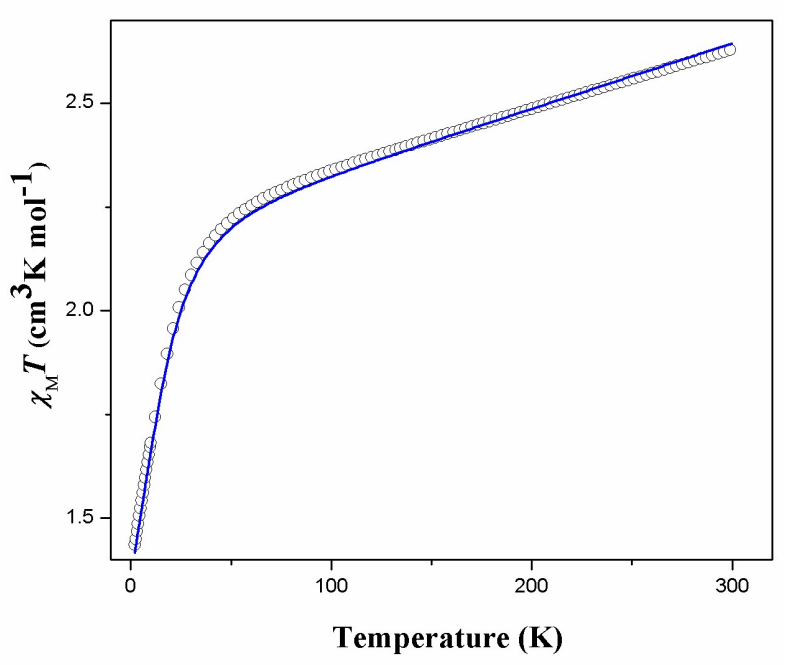

Fig. S23 Plot of $\chi_M T$ *vs. T* for **2**. The circles are the experimental data and the solid line (blue) is generated from the fitted curve.

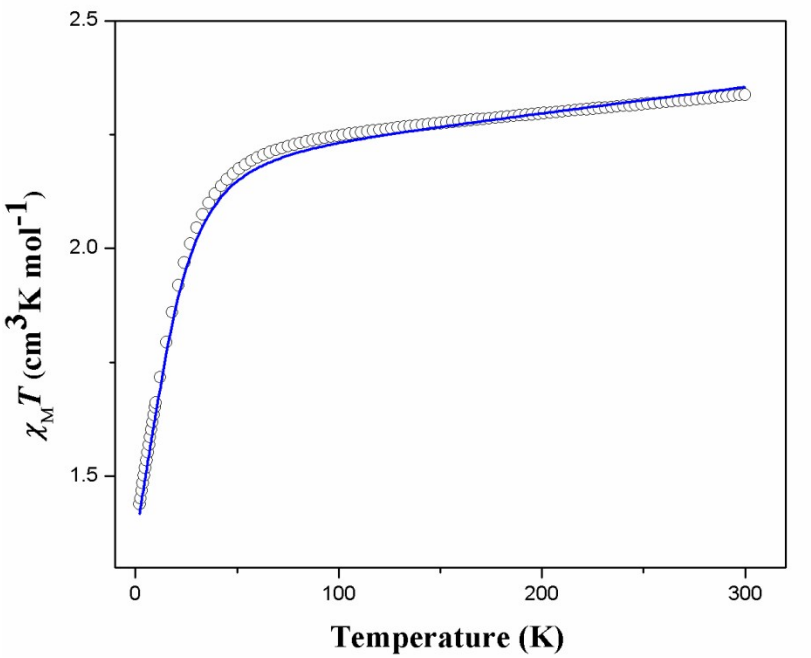

Fig. S24 Plot of $\chi_M T$ *vs. T* for **3**. The circles are the experimental data and the solid line (blue) is generated from the fitted curve.